Available online at www.sciencedirect.com
SCIENCE DIRECT®
Wave Motion 40 (2004) 163–172
WAVE MOTION
www.elsevier.com/locate/wavemoti

Wave scattering by surface-breaking cracks and cavities

Bair V. Budaev*, David B. Bogy

Department of Mechanical Engineering, University of California, Berkeley, CA 94720-1740, USA

Received 18 July 2003; received in revised form 15 January 2004; accepted 6 February 2004

Available online 16 March 2004

Abstract

Here we suggest a new approach to the analysis of two-dimensional wave scattering by arbitrarily shaped irregularities of a boundary of the half-space. This approach employs the probabilistic method of a rigorously justified representation of the scattered waves by explicit formulas involving the computation of mathematical expectations which average the values of certain functionals computed along the trajectories of the random motion governed by specified stochastic differential equations. As typical for the random walk method, the obtained solutions admit numerical implementations by simple algorithms which are practically independent of the particular geometry of the scatterer, which are inexpensive in terms of computer memory requirements, and which have virtually unrestricted capability for parallel processing. Illustrative numerical examples include problems of wave scattering by a tilted straight crack and by a circular cavity.

1. Introduction

The diffraction of waves by a localized irregularity of a flat boundary of the half-space is a phenomenon of considerable interest for various branches of science and engineering including, but not limited to, electromagnetic theory, acoustics, and non-destructive evaluation. However, despite its considerable attention, the arsenal of methods available for the quantitative analysis of this phenomenon remains relatively limited even in the cases that may be formulated as two-dimensional scalar problems for the Helmholtz equations with a constant wave number.

Most of the results available in this area are related to the plane problem of wave scattering by a straight crack orthogonal to the boundary of the half-plane, which is explained by the possibility of symmetrical continuation of such a configuration to the entire plane with a straight slit. The simple geometry of the slit makes it possible to describe waves generated in its exterior by a number of distinctively different methods. Thus, the observations that the Helmholtz equation admits separation of variables in elliptic coordinates and that the slit is an infinitely thin ellipse suggest that the scattered wave can be represented by an infinite series with the terms expressed through Mathieu functions. Another approach explores the physically clear idea of multiple diffractions by the slit's edges. This idea has been implemented by various techniques resulting in exact or approximate solutions tailored for specific needs, such as for the analysis of scattering by a short or, oppositely, by a long crack. To avoid bias in citing original work dispersed in a vast literature covering very different fields, we mention only the collection [1, Chapter 4] which presents a bibliography and review of many important contributions to the topic.

* Corresponding author. Tel.: +1-510-6435776; fax: +1-510-6436162.
E-mail addresses: budaev@me.berkeley.edu, budaev@cml.me.berkeley.edu (B.V. Budaev), dbogy@cml.me.berkeley.edu (D.B. Bogy).

0165-2125/$ – see front matter
doi:10.1016/j.wavemoti.2004.02.003

The methods that exploit the facts that the crack is straight and is orthogonal to the boundary of the half-plane are not easily generalized to handle more complicated geometries, even such as a tilted straight crack, not to mention a curvilinear crack or a cavity of arbitrary shape. In these cases the analytical methods fail and most of the existing approaches are based on the reduction of the problem, by one way or another, to some integral equations that are treated by different numerical schemes. A review of work concerned with the analysis of scattering by curvilinear cracks by integral equations is presented in the paper [7], which itself employs the 'crack Green's function' method leading to a Fredholm integral equation of the second kind with a continuous kernel.

Here we suggest a new approach to the analysis of two-dimensional wave scattering by arbitrarily shaped irregularities of the boundary of the half-space. This approach employs the probabilistic method presented in [2–4] of a rigorously justified representation of the scattered waves by explicit formulas involving the computation of mathematical expectations that average the values of certain functionals computed along the trajectories of random motions governed by specified stochastic differential equations. As typical for the random walk method, the obtained solutions admit numerical implementations by simple algorithms which are practically independent the particular geometry of the scatterer, which are inexpensive in terms of computer memory requirements, and which have virtually unrestricted capability for parallel processing.

In Section 2 we formulate mathematical problems describing scattering of a two-dimensional harmonic wave in a homogeneous half-space damaged by a perturbation of its boundary. First, we specify a boundary-value problem for the homogeneous Helmholtz equation in a damaged half-plane. Next, this problem is transformed to an equivalent one which is considered in the standard half-plane but involves a more complicated Helmholtz equation with a variable wave number. In Section 3 the solution of the latter problem is represented by explicit probabilistic formulas obtained by the random walk method developed in [3,4]. Then, in Section 4 the general solution is applied to the problem of scattering by a tilted crack, and in Section 5 it is applied to the problem of scattering by a meniscus-shaped cavity.

2. Formulation of the scattering problem

Let (ϱ, ϑ) be polar coordinates and let $G = \mathbb{R}^2_+ \setminus \Gamma$ be a half-space $\mathbb{R}^2_+ = \{\varrho, \vartheta : \varrho > 0, 0 < \vartheta < \pi\}$ with the scatterer Γ breaking its boundary. To avoid a lengthy discussion of the class of permissible scatterers, at this point we just mention that it includes, although is not limited to, a straight tilted crack or a circular meniscus-shaped cavity, which are shown in Fig. 1, and will be described in detail later in the part of the paper devoted to the examples illustrating the obtained solutions.

The problem of scattering of the plane wave

$$\mathcal{U}_{\mathrm{i}}(\varrho, \vartheta) = \mathrm{e}^{-\mathrm{i}k\varrho\cos(\vartheta-\vartheta_0)}, \quad 0 < \vartheta_0 < \pi, \tag{2.1}$$

in the domain G is formulated as the computation of the total wave field $\mathcal{U}_{\mathrm{tot}}(\varrho, \vartheta)$ which has to obey the Helmholtz equation, vanish on the boundary ∂G and contain no waves arriving from infinity, except for the incident wave $\mathcal{U}_{\mathrm{i}}(r, \theta)$. Then, selecting an approximate solution $\mathcal{U}_0(r, \theta)$ defined as a wave field which vanishes on a plain part $\partial G \setminus \partial\Gamma$ of the boundary of G, we reduce the problem to that of the computation of the sum

$$\mathcal{U}_{\mathrm{tot}}(\varrho, \vartheta) = \mathcal{U}_0(\varrho, \vartheta) + \mathcal{U}_{\mathrm{s}}(\varrho, \vartheta), \tag{2.2}$$

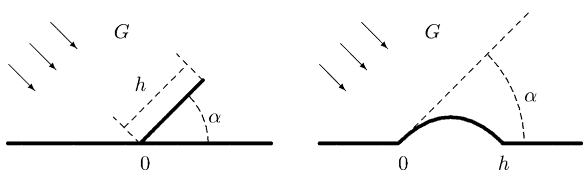

Fig. 1. Samples of permissible domains G.

whose unknown component $\mathcal{U}_s(\varrho, \vartheta)$ has to satisfy the Helmholtz equation

$$\nabla^2 \mathcal{U}_s(\varrho, \vartheta) + k^2 \mathcal{U}_s(\varrho, \vartheta) = 0 \quad (\varrho, \vartheta) \in G, \tag{2.3}$$

accompanied by the radiation condition and by the boundary conditions

$$\mathcal{U}_s|_{\partial \Gamma_*} = -\mathcal{U}_0(\varrho, \vartheta), \tag{2.4}$$

set on the common part $\partial\Gamma_* = \partial G \cap \partial\Gamma$ of the boundaries of G and of the scatter Γ.

It is clear that the approximation $\mathcal{U}_0(\varrho, \vartheta)$ can always be defined as the difference

$$\mathcal{U}_0(\varrho, \vartheta) = \mathcal{U}_i(\varrho, \vartheta) - \mathcal{U}_i(\varrho, -\vartheta), \tag{2.5}$$

but this universal choice is not unique and for many particular scatterers alternative selections of $\mathcal{U}_0(r, \theta)$ may be easily suggested.

To address the problem (2.3) and (2.4) it is convenient to introduce a complex variable $\zeta = \varrho\, e^{i\vartheta}$ so that G can be identified with a domain on the complex plane ζ and, therefore, can be generated from the half-plane $\mathrm{Im}(z) > 0$ by a conformal mapping $z \to \zeta(z)$ fixed by the condition $\zeta(z) = z + o(1)$ as $z \to \infty$. Then, by writing $z = r\, e^{i\theta}$ we obtain new coordinates (r, θ) which have the following important properties:

(a) in the coordinates (r, θ) the domain G is described by the inequality

$$G: \quad r > 0, \quad 0 < \theta < \pi; \tag{2.6}$$

(b) at infinity the coordinates (r, θ) and (ϱ, ϑ) are related by

$$r = \varrho + o(1), \quad \varrho \to \infty; \tag{2.7}$$

(c) the Laplace operators in the coordinates (ϱ, ϑ) and (r, θ) are related by

$$\nabla^2 \mathcal{U}_s(\varrho, \vartheta) = \mu^{-2}(r, \theta) \nabla^2 U_s(r, \theta), \tag{2.8}$$

where

$$U_s(r, \theta) = \mathcal{U}_s(\varrho(r, \theta), \vartheta(r, \theta)), \tag{2.9}$$

and

$$\mu(r, \theta) = |\zeta'(z)|, \quad z = r\, e^{i\theta}. \tag{2.10}$$

In the new coordinates (r, θ) the problem (2.3)–(2.5) is reduced to the Helmholtz equation with a variable wave number

$$\nabla^2 U_s(r, \theta) + k^2 \mu^2(r, \theta) U_s(r, \theta) = 0, \quad r > 0, \ \ 0 < \theta < \pi, \tag{2.11}$$

which has to be solved in the half-plane $r > 0$, $0 < \theta < \pi$ with the boundary conditions

$$U_s(r, 0) = F_0(r), \qquad U_s(r, \pi) = F_1(r), \tag{2.12}$$

whose right-hand sides

$$F_n(r) = -\mathcal{U}_0(\varrho(r, \pi n), \vartheta(r, \pi n)), \quad n = 0, 1, \tag{2.13}$$

are explicitly defined through the pre-defined auxiliary function $\mathcal{U}_0(\varrho, \vartheta)$ from (2.2) and (2.4).

Comparing problems (2.3), (2.4) and (2.11), (2.12) which are equivalent to each other but are formulated in different coordinates (ϱ, ϑ) and (r, θ), respectively, we observe that the complication of the governing equations in the coordinates (r, θ) is offset by the simplification of the problem's geometry, which, as shown in the next section, makes it possible to obtain an explicit probabilistic solution of the problem under investigation.

3. Probabilistic solution of the scattering problem

We seek the solution of the problem (2.11), (2.12) in the product form

$$U_s(r,\theta) = u_s(r,\theta)\,e^{ikr}, \tag{3.1}$$

whose phase $S = kr$ satisfies the equation $(\vec{\nabla} S)^2 = k^2$ and whose amplitude $u_s(r,\theta)$ is considered as a new unknown function which has to obey the complete transport equation

$$\frac{1}{2}\nabla^2 u_s + ik\frac{\partial u_s}{\partial r} + \frac{ik}{2}\left(\frac{1}{r} + ik - ik\mu^2\right)u_s = 0, \tag{3.2}$$

and the boundary conditions

$$u_s(r,\pi n) = F_n(r)\,e^{-ikr}, \quad n = 0, 1, \tag{3.3}$$

equivalent to (2.11) and (2.12).

The problem (3.2) and (3.3) consists of the homogeneous differential equation with analytic coefficients and non-homogeneous boundary conditions whose data functions $F_0(r,\theta)$ and $F_1(r,\theta)$ are not necessarily analytic. However, a simple transformation makes it possible to convert this problem to a more convenient problem with all analytic data.

Consider the function

$$V_x(r,\theta) = \tfrac{1}{2}ikH_1^{(1)}(kr_x)\,e^{-ikr_x}\sin\theta_x, \tag{3.4}$$

where

$$r_x = \sqrt{r^2 - 2rx\cos\theta + x^2}, \qquad \sin\theta_x = \frac{r\sin\theta}{r_x}, \tag{3.5}$$

and x is a real-valued parameter. It is clear that the pair (r_x, θ_x) may be regarded as the coordinates of the point (r,θ) in the polar system centered at (r_*, θ_*) with $r_* = |x|$ and $\theta_* = \arccos(x/|x|)$. Then, the properties of the Hankel functions imply that $V_x(r,\theta)$ obeys the equation

$$\frac{1}{2}\nabla^2 V_x + ik\frac{\partial V_x}{\partial r_x} + \frac{ik}{r_x}V_x = 0, \tag{3.6}$$

and the boundary conditions

$$V_x(r,\theta)|_{\sin\theta=0} = \delta(r\cos\theta - x), \tag{3.7}$$

which guarantee that the integral

$$u_s^0(r,\theta) = \int_{-\infty}^{\infty} V_x(r,\theta) f(x)\,dx, \tag{3.8}$$

has the boundary values $u_s^0(r,0) = f(r)$ and $u_s^0(r,\pi) = f(-r)$. As a results, assigning $f(x)$ as

$$f(x) = \begin{cases} F_0(|x|)\,e^{-ik|x|} & \text{if } x \geq 0, \\ F_1(|x|)\,e^{-ik|x|} & \text{if } x < 0 \end{cases} \tag{3.9}$$

with $F_0(x)$ and $F_1(x)$ from (3.3), we can represent the solution $u_s(r,\theta)$ of the problem (3.2), (3.3) in the form

$$u_s(r,\theta) = u_s^0(r,\theta) + u(r,\theta), \tag{3.10}$$

where $u_s^0(r,\theta)$ is defined by (3.8), (3.9) and $u(r,\theta)$ is the wave field satisfying the homogeneous boundary conditions $u(r,0) = u(r,\pi) = 0$ and the non-homogeneous equation

$$\frac{1}{2}\nabla^2 u + ik\frac{\partial u}{\partial r} + \frac{ik}{2}\left(\frac{1}{r} - ik\chi\right)u + \frac{\Phi}{r^2} = 0, \tag{3.11}$$

where

$$\chi(r,\theta) = \mu^2(r,\theta) - 1, \tag{3.12}$$

and

$$\Phi(r,\theta) = \Phi_0(r,\theta) + \Phi_1(r,\theta) \tag{3.13}$$

is the sum of two pre-defined terms

$$\Phi_0(r,\theta) = \frac{\mathrm{i}kr^2}{2}\int_{-\infty}^{\infty}\left[\left(\frac{1}{r}-\frac{1}{r_x}\right) - \mathrm{i}k\chi(r,\theta)\right] V_x(r,\theta) f(x)\,\mathrm{d}x, \tag{3.14}$$

$$\Phi_1(r,\theta) = \mathrm{i}kr^2\int_{-\infty}^{\infty}\left[\frac{\partial V_x(r,\theta)}{\partial r} - \frac{\partial V_x(r,\theta)}{\partial r_x}\right] f(x)\,\mathrm{d}x, \tag{3.15}$$

each of which is analytic with respect to both arguments r and θ.

Finally, evaluating $\nabla^2 u$ in polar coordinates (r,θ) we convert (3.11) to the equation

$$\frac{r^2}{2}\frac{\partial^2 u}{\partial r^2} + r\left(\frac{1}{2} + \mathrm{i}kr\right)\frac{\partial u}{\partial r} + \frac{1}{2}\frac{\partial^2 u}{\partial \theta^2} + \frac{\mathrm{i}kr}{2}(1-\mathrm{i}kr\chi)u + \Phi = 0, \tag{3.16}$$

which has to be solved in the half-space $r > 0$, $0 < \theta < \pi$ subject to the boundary conditions

$$u(r,0) = u(r,\pi) = 0. \tag{3.17}$$

Equations of the type (3.16) were discussed in [3–5] where it was shown that the solution of the Dirichlet problem (3.16), (3.17) can be represented by either of two equivalent formulas

$$u(r,\theta) = \mathbf{E}\left\{\int_0^{\tau} \Phi(\vec{\xi}_{\mathrm{t}}) \exp\left(\frac{1}{2}\int_0^t (k\xi_{\mathrm{s}}^1)^2\chi(\vec{\xi}_{\mathrm{s}})\,\mathrm{d}s + \mathrm{i}k\xi_{\mathrm{s}}^1\,\mathrm{d}s\right)\mathrm{d}t\right\}, \tag{3.18}$$

or

$$u(r,\theta) = \frac{1}{\sqrt{kr}}\mathbf{E}\left\{\int_0^{\tau} \Phi(\vec{\xi}_{\mathrm{t}})\sqrt{k\xi_{\mathrm{t}}^1} \exp\left(\frac{1}{2}\int_0^t (k\xi_{\mathrm{s}}^1)^2\chi(\vec{\xi}_{\mathrm{s}})\,\mathrm{d}s - \mathrm{d}w_{\mathrm{s}}^1\right)\mathrm{d}t\right\} \tag{3.19}$$

with the mathematical expectations computed overall possible trajectories of the two-component random motion $\vec{\xi}_{\mathrm{t}} = (\xi_{\mathrm{t}}^1, \xi_{\mathrm{t}}^2)$, running in the complex space $\mathbb{C}^2$ under the following rule: the motion starts at the time $t = 0$ from the observation point $\vec{\xi}_0 = (r,\theta)$; it runs thereafter governed by the stochastic differential equations

$$\mathrm{d}\xi_{\mathrm{t}}^1 = \xi_{\mathrm{t}}^1\,\mathrm{d}w_{\mathrm{t}}^1 + \xi_{\mathrm{t}}^1(\tfrac{1}{2} + \mathrm{i}k\xi_{\mathrm{t}}^1)\,\mathrm{d}t, \quad \xi_0^1 = r, \tag{3.20}$$

$$\mathrm{d}\xi_{\mathrm{t}}^2 = \mathrm{d}w_{\mathrm{t}}^2, \quad \xi_0^2 = \theta, \tag{3.21}$$

where w_{t}^1 and w_{t}^2 are independent one-dimensional Brownian motions (Wiener processes); and the motion stops at the exit time $t = \tau$ when its angular component ξ_{t}^2 reaches either of the boundary points $\xi_\tau^2 = 0$ or $\xi_\tau^2 = \pi$.

Eq. (3.11) implies that ξ_{t}^2 is the standard one-dimensional Brownian motion on the real axis, while Eq. (3.20) determines a more complicated random motion inside the quadrant $\mathrm{Re}(\xi_{\mathrm{t}}^1) > 0$, $\mathrm{Im}(\xi_{\mathrm{t}}^1) > 0$ of the complex plane. To verify the last statement we observe that ξ_{t}^1 can neither leave nor reach the axis $\mathrm{Re}(\xi_{\mathrm{t}}^1) = 0$ because, due to (3.20), the differential $\mathrm{d}\xi_{\mathrm{t}}^1$ has purely imaginary values on this axis. Similarly, ξ_{t}^1 cannot leave the quarter-plane $\mathrm{Re}(\xi_{\mathrm{t}}^1) > 0$, $\mathrm{Im}(\xi_{\mathrm{t}}^1) > 0$ through the horizontal semi-axis $\xi_{\mathrm{t}}^1 > 0$, where $\mathrm{d}\xi_{\mathrm{t}}^1$ has a positive imaginary part. Additional information about the motion ξ_{t}^1 comes from the observation [3,4] that it has a drift along the lines

$$\xi_{\mathrm{t}}^1 = \frac{\mathrm{i}r}{2kr - (2kr - \mathrm{i})\,\mathrm{e}^{-t/2}}, \quad t \geq 0, \tag{3.22}$$

all of which, independent of the initial point $\xi_0^1 = r > 0$, run toward the end-point $\xi_\infty^1 = \mathrm{i}/2k$. Combining the above-mentioned details about ξ_{t}^1 we conclude that this motion is localized in the quarter-plane $\mathrm{Re}(\xi_{\mathrm{t}}^1) > 0$,

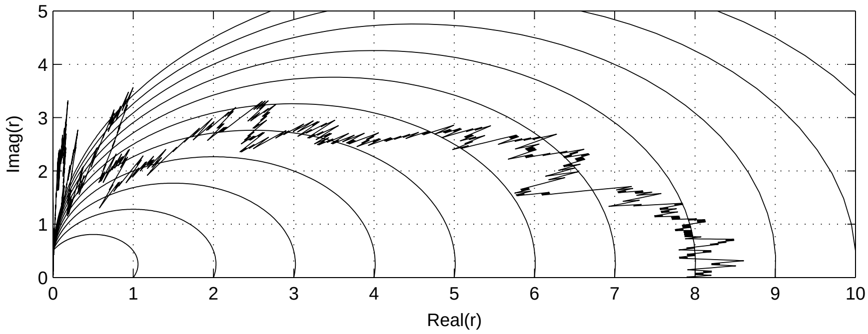

Fig. 2. A sample of the radial random motion $r = \xi_t^1$.

$\mathrm{Im}(\xi_t^1) > 0$, and that the drift drags ξ_t^1 towards the point $\xi_\infty^1 = \mathrm{i}/2k$, so that as $t \to \infty$ the motion ξ_t^1 appears as a random walk in the vicinity of ξ_∞^1. A sample of such motion corresponding to the parameter $k = 1$ is shown by the irregular line in Fig. 2, which also shows smooth oval-shaped lines (3.22) along which the random motion ξ_t^1 drifts.

4. Scattering by a tilted crack

As the first illustration of the obtained results we consider scattering of the plane incident wave

$$\mathcal{U}_\mathrm{i}(\varrho, \vartheta) = \mathrm{e}^{-\mathrm{i}kr\cos(\vartheta-\vartheta_0)}, \quad 0 < \vartheta < \pi, \tag{4.1}$$

propagating in the half-space $\varrho > 0$, $0 < \vartheta < \pi$ damaged by the tilted surface-breaking crack

$$\Gamma \equiv \Gamma_{h,\alpha} = \{\varrho, \vartheta : 0 < r < h, \theta = \alpha\}, \tag{4.2}$$

of the length h and the inclination α, as shown on the left diagram of Fig. 1.

Following the scheme developed in Sections 2 and 3 we begin by introducing new coordinates (r, θ) related to the original polar coordinates (ϱ, ϑ) as

$$z = r\,\mathrm{e}^{\mathrm{i}\theta} \leftrightarrow \varrho\,\mathrm{e}^{\mathrm{i}\vartheta} = \zeta, \tag{4.3}$$

where

$$\zeta(z) = (z-a)^\gamma (z+b)^{1-\gamma} \tag{4.4}$$

is an analytic function with the parameters

$$\gamma = \frac{\alpha}{\pi} < 1, \qquad a = h\left(\frac{\gamma}{1-\gamma}\right)^{1-\gamma}, \qquad b = h\left(\frac{1-\gamma}{\gamma}\right)^{\gamma}, \tag{4.5}$$

which provides the one-to-one conformal mapping of the half-plane $\mathrm{Im}(z) > 0$ to the domain G normalized by the asymptote $\zeta = z + \mathrm{o}(1)$, as $z \to \infty$. Then, the coordinates (r, θ) satisfy all of the conditions (2.6)–(2.8) with the factor $\mu(r, \theta)$ defined by

$$\mu^2(r, \theta) = \zeta'(r\,\mathrm{e}^{\mathrm{i}\theta})\zeta'(r\,\mathrm{e}^{-\mathrm{i}\theta}), \tag{4.6}$$

where

$$\zeta'(z) = \gamma\left(\frac{z+b}{z-a}\right)^{1-\gamma} + (1-\gamma)\left(\frac{z-a}{z+b}\right)^{\gamma}. \tag{4.7}$$

In the new coordinates (r, θ) the tip of the crack corresponds to the point $r = 0$, the right-hand side of the crack corresponds to the segment $0 < r < a$, $\theta = 0$, and the left side of the crack corresponds to the segment $0 < r < b$, $\theta = \pi$.

Next, we need to select an appropriate first approximation $\mathcal{U}_0(\varrho, \vartheta)$ satisfying conditions

$$\mathcal{U}_0(\varrho, 0) = \mathcal{U}_0(\varrho, \pi) = 0, \quad \varrho > 0, \tag{4.8}$$

imposed on the plain part of the boundary ∂G. Obviously, such a function can be defined by the generic formula

$$\mathcal{U}_0(r, \theta) = \mathrm{e}^{-\mathrm{i}k\varrho\cos(\vartheta-\vartheta_0)} - \mathrm{e}^{-\mathrm{i}k\varrho\cos(\vartheta+\vartheta_0)}, \tag{4.9}$$

suggested by (2.5). Then, passing through (2.11)–(2.13), (3.1)–(3.15), we arrive at the Dirichlet problem (3.16), (3.17) whose data-function $\Phi(r, \theta)$ is determined by the expressions (3.13)–(3.15) depending on the function $f(r)$, which degenerates, in the considered particular case, to

$$f(x) = \begin{cases} -2\mathrm{i}\,\mathrm{e}^{-\mathrm{i}kx-\mathrm{i}k\hat{\varrho}\cos\hat{\vartheta}\cos\vartheta_0}\sin(k\hat{\varrho}\sin\hat{\vartheta}\sin\vartheta_0) & \text{if } x \in (-b, a), \\ 0 & \text{if } x \notin (-b, a), \end{cases} \tag{4.10}$$

where

$$\hat{\varrho} = \varrho(|x|, \arg(x)), \qquad \hat{\vartheta} = \vartheta(|x|, \arg(x)), \quad \arg(x) = \begin{cases} 0 & \text{if } x \geq 0, \\ \pi & \text{if } x < 0. \end{cases} \tag{4.11}$$

Finally, the probabilistic formulas (3.18)–(3.21) determine the solution $u(r, \theta)$ of the problem (3.16), (3.17), and the subsequent application of (3.10), (3.1), (2.9) and (2.2) delivers the solution $\mathcal{U}_{\mathrm{tot}}(r, \theta)$ of the original problem of wave scattering by the tilted straight crack.

To illustrate the feasibility of the probabilistic approach to the analysis of wave scattering by a tilted crack we ran two series of simulations based on the obtained solution. In the first series, we successfully considered the scattering of the plane wave (4.1) with incidence angles $\vartheta_0 = 90^\circ$, 120°, 135°, and 150° by the symmetrically oriented crack of length $h = 1$ and of inclination $\alpha = 90^\circ$. In the second series we considered the scattering of the plane wave with incidence angles $\vartheta_0 = 45^\circ$, 90° and 135° by the asymmetrically oriented crack of length $h = 1$ and the inclination $\alpha = 45^\circ$. In both series the scattered field $\mathcal{U}_{\mathrm{s}}(\varrho, \vartheta)$ was computed along the semi-circle $\varrho = 5$, $0^\circ < \vartheta < 180^\circ$.

The results of the probabilistic simulation of scattering by the normal crack are shown in Fig. 3 and similar results corresponding to the 45°-tilted crack are shown in Fig. 4. The simulations were based on the representation (3.19) with the mathematical expectation approximated by the averaging of 3000 discrete random walks with the spatial step $\epsilon = 0.1$. The results were stable with standard deviations at about the 5% level throughout all the experiments.

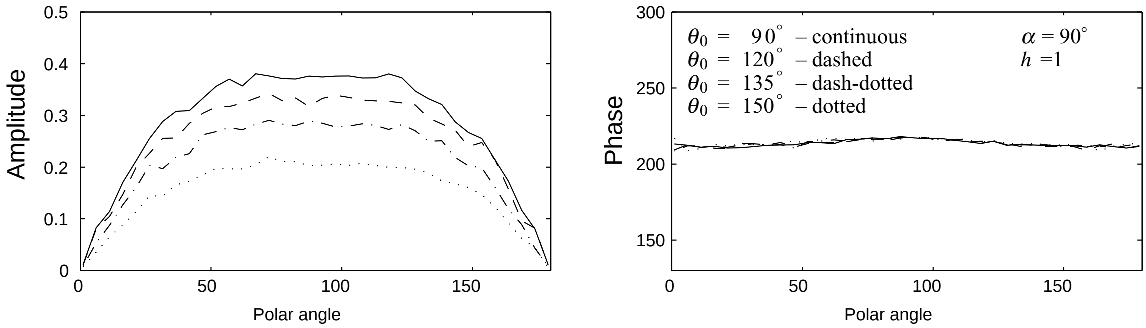

Fig. 3. Scattering by the normal crack, amplitude $|\mathcal{U}_{\mathrm{s}}|$ and phase $\arg(\mathcal{U}_{\mathrm{s}})$.

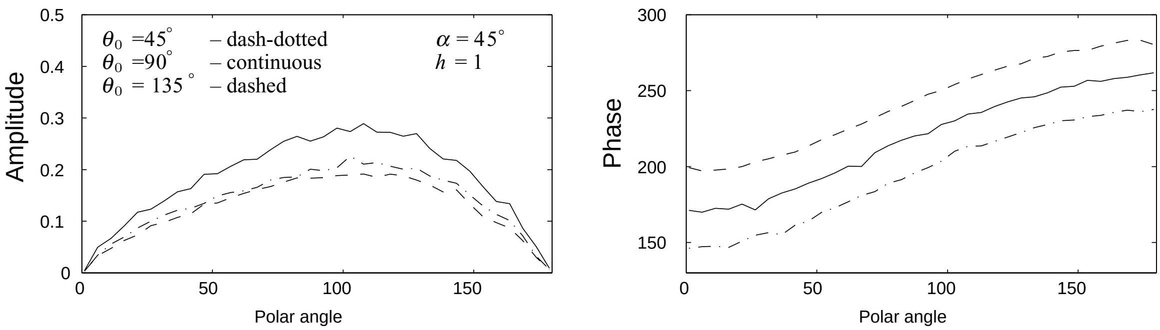

Fig. 4. Scattering by the 45°-tilted crack, amplitude $|\mathcal{U}_s|$ and phase $\arg(\mathcal{U}_s)$.

In conclusion of the discussion of wave scattering by a tilted crack it is instructive to notice that instead of defining the initial approximation $\mathcal{U}_0(r,\theta)$ by the generic formula (4.9) it may be defined by a more sophisticated expression

$$\mathcal{U}_0(r,\theta) = \mathcal{S}_{h,\alpha}(\varrho,\theta;\vartheta_0) - \mathcal{S}_{h,\alpha}(\varrho,-\vartheta;\theta_0), \tag{4.12}$$

where $\mathcal{S}_{h,\alpha}(\varrho,\vartheta;\vartheta_0)$ denotes the wave field generated in the entire space (ϱ,ϑ) due to the scattering of the incident wave (4.1) by the semi-infinite screen continuing the crack $\Gamma_{h,\alpha}$ in the direction $\vartheta=\pi+\alpha$. To compute $\mathcal{S}_{h,\alpha}(\varrho,\vartheta;\vartheta_0)$ it suffices to use the polar coordinates $(\varrho_{h,\alpha},\vartheta_{h,\alpha})$ centered at the vertex of the crack $\Gamma_{h,\alpha}$ and related to (ϱ,ϑ) as

$$\varrho_{h,\alpha} = \sqrt{\varrho^2 - 2\varrho h\cos(\vartheta-\alpha) + h^2}, \qquad \vartheta_{h,\alpha} = \arcsin\left(\frac{r\sin(\vartheta-\alpha)}{\varrho_{h,\alpha}}\right). \tag{4.13}$$

Then, observing that in the coordinates $(\varrho_{h,\alpha},\vartheta_{h,\alpha})$ the incident wave (4.1) has the form of a plane wave $\mathcal{U}_i = \mathrm{e}^{-ik\varrho_{h,\alpha}\cos(\vartheta_{h,\alpha}-\vartheta_0+\alpha)}$, we find that

$$\mathcal{S}_{h,\alpha}(\varrho,\theta;\vartheta_0) = S(\varrho_{h,\alpha},\vartheta_{h,\alpha};\vartheta_0-\alpha), \tag{4.14}$$

where $S(\varrho,\vartheta;\vartheta_0)$ is the well-known [1,6] solution of the classical two-dimensional Sommerfeld problem of diffraction of a plane wave $\mathrm{e}^{ik\varrho\cos(\vartheta-\vartheta_0)}$ by the semi-infinite screen $\vartheta=\pi$. Obviously, formulas (4.12)–(4.14) provide a better initial approximation than (4.9) to the scattered field $\mathcal{U}_s(\varrho,\vartheta)$, but since they are also much more complicated, the use of the simpler formulas (4.9) might be advantageous, at least in cases when the crack is not very long.

5. Scattering by a meniscus-shaped cavity

For the next example we consider scattering of the plane incident wave

$$\mathcal{U}_i(\varrho,\vartheta) = \mathrm{e}^{-ikr\cos(\vartheta-\vartheta_0)}, \quad 0<\vartheta<\pi, \tag{5.1}$$

propagating in the half-space $\mathbb{R}^2_+ = \{\varrho,\vartheta : \varrho>0, 0<\vartheta<\pi\}$ damaged by a cavity Γ which has a shape of a circular meniscus passing through the points $(\varrho,\vartheta)=(h/2,0)$ and $(\varrho,\vartheta)=(h/2,\pi)$ where it intersects the boundary of $\mathbb{R}^2_+$ at the angle α, as shown in Fig. 1.

In this case, the coordinates (r,θ) satisfying conditions (2.6)–(2.8) are introduced by the conformal mapping

$$z = r\,\mathrm{e}^{i\theta} \leftrightarrow \varrho\,\mathrm{e}^{i\vartheta} = \zeta, \tag{5.2}$$

where

$$\zeta(z) = \frac{h}{2}\frac{(z+\gamma h/2)^{1/\gamma} + (z+\gamma h/2)^{1/\gamma}}{(z+\gamma h/2)^{1/\gamma} - (z+\gamma h/2)^{1/\gamma}}, \qquad z(\zeta) = \frac{h\gamma}{2}\frac{(z+h/2)^{\gamma} + (z+h/2)^{\gamma}}{(z+h/2)^{\gamma} - (z+h/2)^{\gamma}}, \tag{5.3}$$

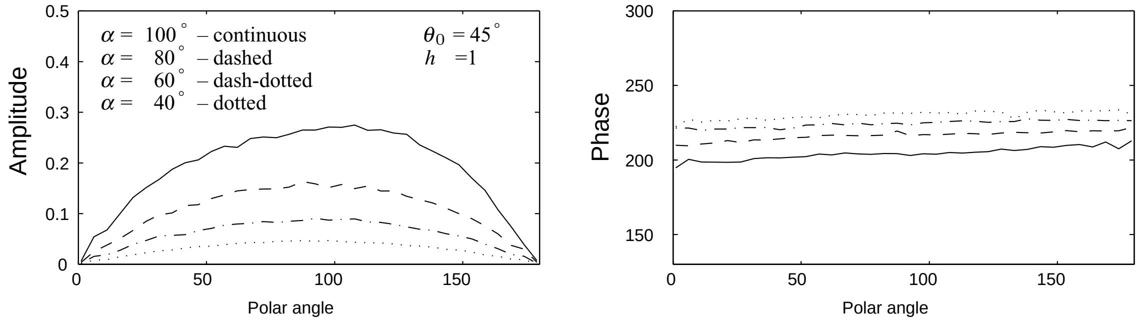

Fig. 5. Scattering by the meniscus-shaped cavity.

are analytic functions inverse to each other and depending on the parameters

$$h \geq 0, \qquad \gamma = \frac{\pi}{\pi - \alpha} > 1, \tag{5.4}$$

characterizing the geometry of the domain G. It is easy to verify that the coordinates (r, θ) satisfy all of the conditions (2.6)–(2.8). Additionally, from (5.2) and (5.3) it is easily seen that the center $\varrho = 0$ of the original coordinates (ϱ, ϑ) coincides with the center $r = 0$ of the new coordinates (r, θ), and that the curvilinear part $\partial\Gamma_*$ of the cavity's boundary is represented in the new coordinates by the simple conditions

$$\partial\Gamma_* : \quad 0 < r < \tfrac{1}{2}\gamma h, \qquad \sin\theta = 0. \tag{5.5}$$

Next, we define the auxiliary function $\mathcal{U}_0(\varrho, \vartheta)$ by the generic formula (2.5) and, passing through (2.11)–(2.13), (3.1)–(3.15), we arrive at the Dirichlet problem (3.16), (3.17) whose data-function $\Phi(r, \theta)$ is defined by the expressions (3.13)–(3.15) depending on the function $f(r)$ which degenerates, in the considered particular case, to

$$f(x) = \begin{cases} -2\mathrm{i}\, \mathrm{e}^{-\mathrm{i}kx - \mathrm{i}k\hat{\varrho}\cos\hat{\vartheta}\cos\vartheta_0} \sin(k\hat{\varrho}\sin\hat{\vartheta}\sin\vartheta_0) & \text{if } x \in \left(-\dfrac{\gamma h}{2}, \dfrac{\gamma h}{2}\right), \\ 0 & \text{if } x \notin \left(-\dfrac{\gamma h}{2}, \dfrac{\gamma h}{2}\right), \end{cases} \tag{5.6}$$

$$\hat{\varrho} = \varrho(|x|, \arg(x)), \qquad \hat{\vartheta} = \vartheta(|x|, \arg(x)). \tag{5.7}$$

After that, the probabilistic formulas (3.18)–(3.21) determine the solution $u(r, \theta)$ of the problem (3.16), (3.17), and the subsequent application of (3.10), (3.1), (2.9) and (2.2) delivers the solution $\mathcal{U}_{\text{tot}}(r, \theta)$ of the original problem of wave scattering by the meniscus-shaped cavity.

Fig. 5 presents the results of the probabilistic simulations of the scattered field $\mathcal{U}_s(\varrho, \vartheta)$ generated by the plane wave (5.1) in the half-plane damaged by the meniscus-shaped cavity characterized by the fixed span $h = 1$ and by the inclination which is subsequently set to four different values $\alpha = 40°, 60°, 80°$, and $100°$. The incidence angle is fixed as $\vartheta_0 = 45°$ and the scattered field is computed along the semi-circle $\varrho = 5$, $0° < \vartheta < 180°$. The simulations were based on the representation (3.19) with the mathematical expectation approximated by the averaging of 3000 discrete random walks with the spatial step $\epsilon = 0.1$. The results were stable with standard deviations at about the 5% level throughout all experiments. To simplify the comparison, Fig. 5 is scaled exactly as Figs. 3 and 4 presenting results of the probabilistic simulation of the scattering by a normal and tilted cracks.

6. Conclusion

In this paper we have considered the two-dimensional problem of wave scattering by an irregularity of the boundary of the half-space. The problem is first transformed, by means of the conformal mapping, to a boundary value problem considered in the undamaged half-plane $\{r, \theta : r > 0, 0 < \theta < \pi\}$, but formulated for the Helmholtz equation $\nabla^2 U_s + k^2\mu^2 U_s = 0$ with the variable factor μ. The solution of the latter problem has been sought in the form $U_s = (u + u_0)\,e^{ikr}$ with the pre-defined term $u_0\,e^{ikr}$ satisfying required boundary conditions and with the new unknown function $u(r, \theta)$ vanishing on the boundary of the half-space and satisfying the complete transport equation

$$\frac{r^2}{2}\frac{\partial^2 u}{\partial r^2} + r\left(\frac{1}{2} + \mathrm{i}kr\right)\frac{\partial u}{\partial r} + \frac{1}{2}\frac{\partial^2 u}{\partial \theta^2} + \frac{\mathrm{i}kr}{2}(1 + \mathrm{i}kr[1 - \mu^2])u = -\Phi$$

with the pre-defined right-hand side function $\Phi(r, \theta)$. Finally, the solution of this equation is found in an explicit probabilistic form which may be considered as an adaptation of the well-known Feynman–Kac formulas to the equation with complex-valued analytic coefficients.

Although the examples considered in the paper are restricted to particular scatterers which are the straight crack and the circular meniscus-shaped cavity, the obtained results clearly show that the version of the random walk methods developed in [3,4] provides a universal solution of the problem of diffraction by an arbitrarily shaped irregularity of the flat boundary of the half-space. As with analytic or asymptotic methods, probabilistic solutions provided by the random walk method are local in the sense that they make it possible to compute functions of interest at individual points without computing them on dense meshes. Moreover, such solutions admit simple implementations which are practically independent on the particular geometry of the scatterer, which are inexpensive in terms of computer memory requirements, and which have virtually unrestricted capability for parallel processing. All of these features together make the random walk method attractive for both qualitative and numerical analysis of wave scattering and suggest that research in this direction should be pursued further, with the aim of creating a simple unified approach for the analysis of wave propagation in non-homogeneous, anisotropic media described by systems of differential equations and sophisticated boundary conditions arising, in particular, from practical problem of continuum mechanics and radio sciences.

Acknowledgements

This research was supported by NSF Grant CMS-0098418 and by the William S. Floyd Jr. Distinguished Professorship in Engineering held by D. Bogy.

References

[1] J.J. Bowman, T.B.A. Senior, P.L.E. Uslenghi (Eds.), Electromagnetic and Acoustic Scattering by Simple Shapes, Hemisphere, New York, 1969.
[2] B.V. Budaev, D.B. Bogy, Application of random walk methods to wave propagation, Quart. J. Mech. Appl. Math. 55 (2) (2002) 209–226.
[3] B.V. Budaev, D.B. Bogy, Diffraction by a plane sector, in: Proceedings of the Royal Society A, in press.
[4] B.V. Budaev, D.B. Bogy, Random walk approach to wave propagation in wedges and cones, J. Acoust. Soc. Am. 114 (4) (2003) 1733–1741.
[5] B.V. Budaev, D.B. Bogy, Random walk approach to wave radiation in cylindrical and spherical domains, Probab. Eng. Mech. 18 (2003) 339–348.
[6] L.B. Felsen, N. Marcuvitz, Radiation and Scattering of Waves, Prentice-Hall Microwaves and Fields Series, Prentice-Hall, Englewood Cliffs, NJ, 1972.
[7] P.A. Lewis, G.R. Wickham, The diffraction of sh waves by an arbitrary shaped crack in two dimensions, Phil. Trans.: Phys. Sci. Eng. 340 (1659) (1992) 503–529.